American Mineralogist, Volume 63, pages 28–36, 1978

The crystal structure of loveringite—a new member of the crichtonite group

BRYAN M. GATEHOUSE

Chemistry Department, Monash University
Clayton, Victoria 3168, Australia

IAN E. GREY

CSIRO, Division of Mineral Chemistry, P.O. Box 124
Port Melbourne, Victoria 3207, Australia

IAN H. CAMPBELL[1] AND PATRICK KELLY

Earth Sciences Department, University of Melbourne
Parkville, Victoria 3052, Australia

Abstract

Loveringite, a new calcium iron titanate, was discovered in the Jimberlana Intrusion near Norseman, Western Australia. The unit-cell composition of the type sample, normalized to 38 oxygens, is $Ca_{0.72}REE_{0.33}(Y,Th,U,Pb)_{0.05}Ti_{12.48}Fe_{3.38}Cr_{2.24}Mg_{0.92}Zr_{0.58}Al_{0.39}V_{0.21}Mn_{0.04}O_{38}$, which may be abbreviated as $AM_{20.34}O_{38}$; A = Σ large cations and M = Σ small cations (including some REE). The mineral contains about 0.2 percent uranium and is metamict in its natural state. The crystal structure of the type grain was reconstituted by heating in air at 800°C. Single-crystal X-ray diffraction studies showed it to have rhombohedral symmetry, $R\bar{3}$, with unit-cell parameters a_{rh} = 9.117(4)A, α_{rh} = 69.07(1)°. The structure was solved using 398 observed [$I \geq 2\sigma(1)$] symmetry-independent reflections, refined to an R value of 0.043. Loveringite is isostructural with senaite and crichtonite, with a structure based on a nine-layer ($hhc\cdots$) close-packed anion lattice in which the A cation occupies an anion site and the M cations are ordered into 19 octahedral and 2 tetrahedral sites per unit cell.

Microprobe analyses for a number of loveringite samples are reported, and the observed compositional variations are discussed in relation to the structure.

Introduction

We have recently reported the crystal structures of the minerals senaite (Grey and Lloyd, 1976) and crichtonite (Grey *et al.*, 1976). These minerals are isostructural and have compositions described by the general formula $AM_{21}O_{38}$, where M = small cations, predominantly Ti and Fe, and A = large cations (mainly Pb in senaite and Sr in crichtonite). The compounds have rhombohedral symmetry, and the structures are based on a close-packed anion lattice with a stacking sequence ($hhc\cdots$) and with the large cations occupying one of the anion sites. The small cations occupy both octahedral and tetrahedral interstices in the close-packed lattice.

As part of a general study on minor phases occurring in the Jimberlana Intrusion near Norseman in Western Australia, we identified a mineral with a composition very similar to that of crichtonite and senaite, but with calcium as the major large cation. An X-ray diffraction study showed that the mineral was metamict, due to radiation damage from the uranium present (approximately 0.2 weight percent UO_2). Crystals reconstituted by careful heat treatment exhibited rhombohedral symmetry with unit-cell dimensions very similar to those for senaite and crichtonite. Its isostructural relationship to these minerals was confirmed by a single-crystal X-ray structure analysis, which is the subject of this paper.

[1] Present address: The Department of Geological Sciences, Queen's University, Kingston, Canada.

0003-004X/78/0102-0028$02.00

Analytical data for a range of samples are also reported.

Occurrence and compositional variation

The mineral loveringite[2] was found during a study of uranium-bearing phases of the Jimberlana Intrusion near Norseman, Western Australia (Campbell and Kelly, in press). The phases were located by the lexan print method (Kleeman and Lovering, 1967), and identified using a scanning electron microscope equipped with a multichannel analyser.

Jimberlana is a layered intrusion which contains a repeated sequence of olivine and bronzite cumulate layers overlain by a thick plagioclase–augite–hypersthene cumulate layer (Campbell *et al.*, 1970). Loveringite is most abundant in bronzite cumulate layers, but even in these rocks it rarely exceeds 5 grains per slide. The mineral is also found in the lower half of the plagioclase–augite–hypersthene cumulate layer, but has not yet been recorded in the olivine cumulates. It occurs as isolated crystals which are usually anhedral but occasionally form needles. The grain size rarely exceeds 100 × 50 μm. The mineral is closely associated with either quartz and K-feldspar intergrowths or phlogopite. Other uranium and rare-earth bearing accessory minerals in the cumulate layers are baddeleyite, apatite, zircon, sphene, and rutile. Ilmenite and chromite are also common.

The compositions of more than thirty grains of loveringite were determined by microprobe analyses. The detailed interpretation of these results will be published elsewhere (Campbell and Kelly, in press). To illustrate the wide ranges of metal-atom substitutions observed, the results of microprobe analyses on five grains are given in Table 1. Sample C116-5, Table 1, was used for the single-crystal *X*-ray diffraction study, after restoration of the crystal structure by heating in air at 800°C. The analysis on this grain was performed after reconstitution, and so the elements are considered to be in the valence states pertaining to the oxidizing conditions used, *i.e.* Fe^{3+}, V^{5+} *etc.* These are shown as oxides in Table 1. The analyses illustrate two main types of isomorphous replacement, *i.e.* iron–chromium and calcium–rare earth. Significant variations in the amounts of titanium (54.6–64.1 weight percent), vanadium (0.5–4.5 weight percent), and zirconium (1.2–6.1 weight percent) were also observed, although these elements showed no obvious replacement correlations with other elements.

The iron–chromium substitution correlates with the position of the mineral in the layering sequence. Loveringite samples taken from the plagioclase-hypersthene layer had negligible chromium contents ($\lesssim$ 0.1 weight percent). At the contact of this layer with the underlying bronzite cumulate layer, the chromium content of the loveringites showed a sudden jump to 3 or 4 weight percent, whereas the iron contents showed a concomitant decrease. All samples taken from the bronzite layer had appreciable substitution of chromium for iron, up to a maximum replacement of about 50 percent of the iron present.

Calcium–rare earth substitution showed a similar trend to iron–chromium, with the samples taken from the plagioclase–hypersthene layer generally displaying the highest calcium–lowest rare earth analyses. Sample C187-31 in Table 1 is an exceptional example of this. It is an almost pure calcium end-member phase, with 94 atom percent contribution of calcium to the large-cations group. This sample was also unique in having the highest vanadium and lowest zirconium contents of all the specimens analysed. Unfortunately, this sample was too small (0.03 mm × 0.01 mm) for X-ray study, and was also damaged during excavation from the surrounding silica matrix.

The compositional variations are discussed in relation to the structure of loveringite in a later section.

Experimental

Natural loveringite has an interesting type of metamict structure, in which there is a breakdown in the metal atom ordering but the close-packed anion lattice remains coherent enough to give a sharp diffraction pattern. Individual grains of the mineral gave single-crystal X-ray diffraction patterns consisting of sharp spots which all indexed on a hexagonal cell, a = 2.87, c = 20.67 A. This corresponds to the strong pseudo-cell observed for crichtonite (Hey *et al.*, 1969), and is due to diffraction from a close-packed anion array with a ($hhc\cdots$) stacking sequence; *i.e.* c_{hex} = 9 × anion layer repeat. The atom displacements induced by radiation are apparently only slight, and a single heating for one hour at 800°C was sufficient to reconstitute the mineral. The resulting single-crystal X-ray patterns were similar to those for senaite and crichtonite. The rhombohedral symmetry was confirmed from precession and Weissenberg photographs.

For the structure determination, a reconstituted

[2] The name for this new mineral and the proposal for the systematic nomenclature of the crichtonite mineral series has been approved by the IMA Commission on New Minerals and New Mineral Names.

Table 1. Microprobe analyses on loveringite samples from Norseman, Western Australia, and davidite from Olary, South Australia

	C116-5 (Data crystal)	C193-2	N138-17	C187-31	RRD4-291-5	Davidite from Olary, South Australia
TiO_2	58.34	59.15	54.67	64.10	55.35	51.74
Al_2O_3	1.15	0.94	0.58	1.54	0.93	0.22
Fe_2O_3	15.77	24.15	26.76	20.84	20.58	25.30
MnO	0.17	0.13	0.03	0.21	0.13	0.04
MgO	2.18	1.22	0.63	0.67	1.36	0.10
CaO	2.37	2.50	3.43	4.54	1.45	0.23
Cr_2O_3	9.94	0.10	0.06	0.15	6.90	1.21
SiO_2	-	0.07	0.57*	1.38	-	-
Na_2O	-	0.06	-	0.13	-	-
K_2O	-	-	-	0.04	-	-
NiO	0.08	0.07	0.11	-	0.03	-
UO_2	0.18	0.17	0.34	-	0.18	6.42
PbO	0.22	0.23	0.15	-	0.05	0.69
HfO_2	0.35	0.20	0.03	0.11	0.16	0.51
ZrO_2	4.18	5.40	6.12	1.21	4.24	0.07
ThO_2	0.09	0.52	0.53	0.09	0.34	0.05
CeO_2	1.28	1.12	1.21	0.26	2.75	3.06
La_2O_3	1.22	0.84	0.78	0.08	2.43	3.35
Nd_2O_3	0.24	0.16	0.42	0.05	0.35	0.35
V_2O_5	1.10	0.94	0.37	4.40	1.41	2.88
Y_2O_3	0.09	0.10	0.14	0.26	0.27	1.86
R.E.E.**	0.26	0.21	0.19	0.03	0.30	0.88
SrO	-	-	-	0.01	-	0.02
Total	99.21	98.28	97.12	100.10	99.21	98.98

*Samples N138-17 and C187-31 measured 0.005 mm x 0.05 mm and 0.01 mm x 0.03 mm respectively. Si and Na contribution from surrounding matrix for these very small crystals.
**Other rare earth contributions estimated from chondrite normalized rare earth patterns.

crystal measuring 0.03 × 0.05 × 0.07 mm was transferred to a Phillips PW1100 4-circle automatic diffractometer. Least-squares refinement of 2θ values obtained for centred high-angle reflections gave the rhombohedral cell parameters a_{rh} = 9.117(4)A, α_{rh} = 69.07(1)°. The corresponding hexagonal parameters are a_{hex} = 10.337, c_{hex} = 20.677A, *i.e.* $\sqrt{13}$ and 1 times the subcell values respectively.

Intensities were collected with graphite monochromated Mo$K\alpha$ radiation with a tower angle of 12.18°. A θ-2θ scan, 3–25°, was used with a variable scan width given by $\Delta\theta = (1.2 + 0.3 \tan \theta)$ and a speed of 0.05° sec^{-1}. Two background measurements, each for half the scan time, were made for each scan, one at the lower and one at the upper limit. The intensities were processed using a program written for the PW1100 diffractometer by Hornstra and Stubbe (1972). Because of the very small size of the crystal ($\mu \cdot R$ = 0.20) an absorption correction was not applied. However, a partial compensation was

achieved by averaging the intensities of equivalent reflections in the rhombohedral cell. Thus the reflections measured were reduced to a unique set of 844 reflections. Due to the very small crystal volume, a large number of reflections were extremely weak. Less than half (398) of the unique reflections had $I \geq 2\sigma$ [I] and were used in the structure refinement.

Scattering-factor curves for Ca, La, Ce, Ti, Fe, Cr, Mg, Zr, Al, V, and O were taken from *International Tables for X-ray Crystallography III* (1962, p. 201ff). The curves for Ce, La, and Zr were corrected for anomalous dispersion. All computing was performed on the Monash University CDC 3200 and the CSIRO CDC 7600 computers.

At the completion of the intensity data collection, the crystal was prepared in a polished mount and analyzed on a JEOL electron microprobe, using a sample current between 0.2 and 0.4 μA with the beam focused to about 5 μm. Most of the elements were measured at 15 kV, but Pb, Hf, Zr, Th, Nd, Ce, La, Y, and Sr were determined at 20 kV. The results of the probe analysis are given in the first column of Table 1 (C116-5). The calculated unit-cell composition normalized to 38 oxygens is $[Ca_{0.72}REE_{0.33}(Y,Th,U,Pb)_{0.05}][Ti_{12.48}Fe_{3.38}Cr_{2.24}Mg_{0.92}Zr_{0.58}Al_{0.39}V_{0.21}Mn_{0.04}]O_{38}$. This may be generalized as $A_{1.10}M_{20.24}O_{38}$, where A = large cations, M = small cations.

Solution and refinements of the structure

The atom coordinates obtained for senaite in the centrosymmetric space group $R\bar{3}$ (Grey and Lloyd, 1976) were used as a starting model for loveringite. In determining the distribution of the cations among the different sites available, we were guided by the results for senaite and crichtonite, which showed ordering sequences based on the size of the cations. Accordingly, composite scattering curves were prepared for the sites in loveringite consisting of Ca + REE in $M(0)$, Mg in $M(1)$, Mg + Fe in $M(2)$ (where the iron is presumably partly Fe^{2+} in the mineral before reconstitution), Cr, V, Fe in $M(3)$, and Ti, Al in $M(4)$, $M(5)$. Tetravalent Zr was included with Ti^{4+} in sites $M(4)$ and $M(5)$.

A number of cycles of full-matrix least-squares refinement led to satisfactory convergence of all positional parameters at a conventional R value of 0.08. However, the isotropic temperature factors showed some serious discrepancies. In particular, $M(1)$ had an associated large negative B value of -1.4, whereas the values for the other metals ranged from 0.3 to 1.5. Transferring all the tetravalent zirconium to site $M(1)$ gave a marked improvement in the B value for this site, although it still remained negative at -0.1, and the R factor dropped to 0.06. A difference Fourier calculated at this stage showed a positive peak corresponding to about 3 electrons at site $M(1)$. This was interpreted in the light of the calculated chemical formula, $A_{1.1}M_{20.24}O_{38}$, where A = Ca + REE + (Y,Th,U,Pb), as indicating some ordering of the A cations into $M(1)$, which is the largest octahedral site in both senaite and crichtonite (Grey *et al.*, 1976). Accordingly, 0.1 REE were ordered with the Zr and Mg into site $M(1)$.

A new set of composite scattering curves for the metal atom sites was prepared, consistent with the unit-cell composition. The deficiency in the number of small cations, $\Sigma M = 20.34$ relative to the number of sites, 21, was met by incorporating vacancies in sites $M(2)$ and $M(3)$. The reason for this is outlined in the discussion. Least-squares refinement of all positional and isotropic thermal parameters gave a final R factor of 0.043 for all observed data. The site occupancies are given in Table 2, together with the refined coordinates and isotropic temperature factors. The observed and calculated structure factors are given in Table 3. Although the site occupancies in Table 2 give compatible size groupings of cations, and lead to satisfactory thermal parameters for all sites, it should be emphasized that they were derived mainly by crystallochemical arguments. Many details are open to debate, *e.g.* the relative distribution of Fe and Mg between sites $M(1)$ and $M(2)$, and the allocation of the fractional occupancy of octahedral and tetrahedral sites, *i.e.* the way in which the 20.34 M cations are distributed among the 21 crystallographic sites. This will correlate strongly with the ordering of similar-sized ions, such as Mg^{2+} and Zr^{4+}, with widely different scattering powers. However, because of the large number of different elements involved in the ordering process, independent least-squares refinement of both temperature factors and site occupancies is not possible, and we are left with crystallochemical reasoning as the only recourse.

Description of the structure

Loveringite is isostructural with senaite and crichtonite. The structure is based on a close-packed anion framework with a nine-layer stacking sequence ($hhc\cdots$) and with the large cations, mainly Ca and REE, occupying anion sites. The small cations occupy octahedral and tetrahedral interstices between the close-packed anion layers. There are two types of cation layers, illustrated in Figures 1 and 2. Metal

Table 2. Loveringite: final atomic coordinates and isotropic temperature factors

Atom Site	Occupancy	X	Y	Z	B ($Å^2$)
M(0)	0.72 Ca + 0.23 R.E.E. + 0.05 (Y, Th, U, Pb)	0.0000	0.0000	0.0000	2.11(11)
M(1)	0.58 Zr + 0.1 R.E.E. + 0.32 Mg	0.5000	0.5000	0.5000	0.77(7)
M(2)	0.60 Mg + 1.23 Fe	0.31090(15)	0.31090(15)	0.31090(15)	0.69(8)
M(3)	2.24 Cr + 2.19 Fe + 0.86 Ti + 0.21 V	0.34754(34)	0.12318(33)	0.02156(34)	0.72(5)
M(4)	5.81 Ti + 0.19 Al	0.30841(36)	0.72081(33)	0.14588(37)	0.63(5)
M(5)	5.81 Ti + 0.19 Al	0.47612(38)	0.08155(35)	0.63977(37)	0.75(5)
O(1)	6.00 O	0.3058(13)	0.6269(13)	0.3801(13)	0.92(19)
O(2)	6.00 O	0.1523(14)	0.2378(14)	0.9393(13)	1.14(21)
O(3)	6.00 O	0.9211(12)	0.4571(12)	0.3002(13)	0.47(15)
O(4)	6.00 O	0.1427(14)	0.5149(14)	0.9908(14)	1.16(17)
O(5)	6.00 O	0.3901(14)	0.4896(14)	0.1345(14)	1.11(18)
O(6)	6.00 O	0.7104(12)	0.2410(12)	0.0699(13)	0.55(16)
O(7)	2.00 O	0.2120(8)	0.2120(8)	0.2120(8)	0.55(33)

*Note reversal of order of Y, Z c.f. that in senaite (Grey and Lloyd, 1976) resulting from opposite direction of unique axis in data collection.

atoms $M(1)$ and $M(3)$ occupy octahedral sites between pairs of hexagonal-stacked anion layers, *i.e.* *h–M–h*, Figure 1, whereas $M(2)$, tetrahedral, and $M(4)$, $M(5)$, octahedral, form *h–M–c* layers between adjacent hexagonal and cubic anion layers, Figure 2. Further structural details are given in the papers on crichtonite (Grey *et al.*, 1976) and senaite (Grey and Lloyd, 1976).

Interatomic distances

Polyhedral bond lengths and angles for loveringite are given in Table 4. The average interatomic distances are very similar to those for both crichtonite and senaite. The greatest change is associated with site $M(1)$. This site is occupied mainly by the large divalent manganese cation in senaite, $M(1)$–O = 2.227A, and crichtonite, $M(1)$–O = 2.205A, whereas in loveringite the major contributor is the smaller tetravalent Zr cation, $M(1)$–O = 2.166A.

Within the associated experimental errors, there is no effective change in the $M(0)$–O distance from senaite, 2.817(17)A, to crichtonite, 2.792(7)A, to loveringite, 2.789(11)A, even though the radius of the dominant large cation changes considerably from 1.49A for lead, to 1.40A for strontium, to 1.35A for calcium (Shannon and Prewitt, 1969). It would thus seem that the $M(0)$–O distance in these compounds is determined mainly by the close-packing of the oxygens. The average oxygen radius is approximated by $0.5a_{hex}\sqrt{13}$, which gives 1.440, 1.439, and 1.436A respectively for senaite, crichtonite, and loveringite, *i.e.* for the latter two cases, the oxygens are somewhat larger than the *A* cations.

Despite the wide ranges of elemental substitutions possible in these minerals as illustrated in Table 1, and also Table 1 in Grey *et al.* (1976), the one constant crystal-chemical feature is the high degree of ordering of tetravalent titanium cations into the octahedral sites $M(4)$ and $M(5)$ within the *h–M–c* layers. This is reflected in their average $M(4)$–O and $M(5)$–O separations, which are 1.976(18) and 1.964(18), 1.969(7) and 1.967(7), and 1.970(11) and 1.970(11)A respectively for senaite, crichtonite, and loveringite. These are identical within experimental error and agree with the average Ti–O distance of 1.96(2) in brookite (Baur, 1961) which also has a mixed (*chch* $\cdots$) stacking of close-packed oxygen layers and with each TiO_6 octahedron sharing three edges. In loveringite, the $M(4)$ and $M(5)$ atoms alternate in six-membered rings of edge-shared octahedra within a *h–M–c* layer as shown in Figure 2, and between pairs of *h–M–c* layers the octahedra also share edges to form clusters of four octahedra as shown in Figure 3(i). Also shown in Figure 3(i) is the linking of the $M(2)O_4$ tetrahedra to the four-octahedra clusters. This particular articulation of polyhedra is actually the basic structure unit for β-Ga_2O_3 (Geller, 1960) and is found in $Ga_4Ti_{21}O_{48}$, which is a rutile–beta gallia intergrowth (Lloyd *et al.*, 1976). In the latter compounds, the edge-sharing of octahedra extends infinitely in one direction to build up double chains as shown in Figure 3(ii). It is interesting that virtually identical values are obtained for the *M–M* separations across shared edges in loveringite and $Ga_4Ti_{21}O_{48}$. In both cases, the inter-chain shared-edge repulsions are considerably greater (loveringite and $Ga_4Ti_{21}O_{48}$, both 3.22A) than the intra-chain *M–M* values (loveringite 2.99, $Ga_4Ti_{21}O_{48}$ 2.97A).

Table 3. Observed and calculated structure factors for loveringite

H	K	L	FO	FC	H	K	L	FO	FC	H	K	L	FO	FC	H	K	L	FO	FC
8	11	9	42,04	40,59	6	4	8	27,24	11,50	1	6	5	74,15	75,05	-1	2	5	99,99	99,08
8	7	11	62,52	65,17	5	8	8	46,82	47,11	5	6	1	69,49	71,21	2	1	5	260,58	240,15
6	11	9	39,44	35,71	8	1	5	68,01	67,69	-5	-6	4	68,87	67,88	2	5	1	22,50	25,06
6	7	11	31,20	25,52	1	4	8	43,57	44,94	-6	-5	4	89,48	89,09	1	1	5	26,38	22,60
6	6	11	61,47	62,77	8	1	1	76,58	76,44	6	4	1	73,41	72,80	0	4	5	23,20	28,44
11	5	10	38,70	32,22	2	6	8	69,74	71,40	1	4	6	68,81	72,06	5	0	3	34,58	31,88
5	11	9	37,09	35,58	5	8	2	80,21	79,45	-5	-6	1	52,14	52,15	3	0	5	24,77	24,31
11	5	9	43,32	44,55	8	4	2	35,12	37,48	-6	-5	1	47,56	49,90	0	5	2	37,71	34,20
5	7	11	49,58	52,30	8	3	4	43,15	41,87	-3	-5	6	36,23	38,47	0	3	5	41,63	64,15
5	6	11	33,06	29,95	0	8	4	27,17	15,90	-2	6	6	47,73	49,80	0	1	5	118,37	120,14
5	5	11	37,22	39,94	3	2	8	29,14	30,14	5	6	2	109,80	111,77	1	0	5	50,04	51,68
8	4	11	32,52	30,54	8	2	3	48,06	46,19	2	6	5	49,67	51,24	0	5	0	130,28	129,62
7	4	11	50,82	46,51	8	3	2	61,49	62,29	-6	-2	4	59,31	58,41	-4	-4	4	83,79	82,07
4	8	11	76,21	73,97	1	6	8	53,62	54,97	-2	4	6	139,76	139,80	-4	-3	4	43,36	41,71
5	4	11	38,12	34,05	1	5	8	74,48	74,80	-2	-4	6	45,13	45,12	-4	-4	3	97,52	96,79
4	5	11	33,96	30,08	1	8	4	25,88	12,93	-4	-2	6	55,56	56,48	-3	-4	3	38,70	40,55
5	3	11	77,73	78,36	1	4	8	27,82	33,02	-2	-6	4	55,15	54,30	-2	-4	4	64,17	61,40
3	5	11	52,47	55,58	-1	3	8	54,61	59,66	2	6	4	29,92	25,45	-2	4	4	116,89	115,63
3	5	11	35,20	39,75	1	3	8	66,36	71,91	-2	-6	3	86,84	86,16	-4	-1	4	26,54	19,03
3	2	11	48,02	55,20	-8	-1	2	27,12	18,58	-6	-3	3	55,35	57,69	-4	0	4	28,69	23,13
2	2	11	30,42	31,66	1	8	2	26,42	26,92	-3	-2	6	46,06	48,00	-2	-2	4	42,29	40,72
1	7	11	38,70	39,28	-1	2	8	34,75	38,99	-2	-3	6	27,82	25,57	-4	-2	2	72,54	72,25
1	6	11	38,45	40,03	-1	8	2	26,05	23,90	2	6	3	219,15	219,85	-2	2	4	93,73	90,74
1	4	11	56,88	54,08	-1	-1	8	27,24	26,64	-2	2	6	58,82	59,47	-2	-4	3	69,41	65,65
3	1	11	31,61	32,22	1	1	8	27,61	17,79	-6	-2	3	77,03	77,59	-4	-3	2	55,64	53,96
1	3	11	34,91	33,54	0	5	8	45,63	40,37	-2	-2	6	36,39	37,68	-3	3	4	62,40	60,33
2	1	11	49,95	51,18	0	8	2	198,58	198,35	2	6	2	63,18	63,69	-3	-1	4	363,40	362,88
4	0	11	55,27	52,85	0	0	8	54,78	50,07	-1	6	6	24,94	20,32	-1	-3	4	90,88	88,18
3	0	11	43,11	44,11	7	7	7	94,01	96,07	-1	5	6	80,21	80,59	-1	-4	3	67,59	67,22
2	0	11	35,03	31,47	6	7	7	39,03	40,38	5	1	6	60,71	62,73	-1	4	3	130,08	126,80
10	4	10	43,24	34,64	7	6	6	33,06	35,83	-1	6	4	64,26	65,27	-1	3	4	22,46	31,54
10	3	10	56,75	52,00	7	5	6	40,47	42,31	-1	-6	4	48,02	47,08	-2	-1	4	40,06	39,72
10	2	10	39,20	38,87	7	6	6	25,22	27,04	-4	-1	6	31,41	31,27	-1	4	2	139,39	136,47
7	10	9	46,78	43,00	7	4	5	95,91	98,22	-6	-1	4	49,58	49,96	-1	4	1	21,93	24,83
7	8	10	48,26	44,15	4	4	7	48,92	50,18	-1	4	6	49,13	48,35	-1	1	4	106,13	103,61
9	6	10	47,56	48,29	8	3	7	90,26	93,15	1	4	6	23,25	22,26	-1	4	0	41,63	40,19
5	10	9	60,01	52,89	6	7	3	29,22	30,47	-1	-6	3	63,23	65,85	-1	0	4	19,95	13,75
4	10	9	42,58	44,40	5	3	7	31,94	31,69	-6	-1	1	79,05	80,35	4	4	4	109,39	112,87
9	1	10	37,55	31,13	7	3	5	32,48	35,24	1	1	6	30,38	31,96	4	3	4	28,85	29,18
9	0	10	63,47	58,54	7	3	6	46,08	48,72	1	6	1	57,99	57,38	4	4	3	56,26	56,55
8	8	10	41,59	44,82	7	4	3	42,99	44,63	-1	-2	6	37,88	37,95	4	0	4	28,32	24,87
8	5	10	62,73	62,64	7	3	3	43,19	44,31	-1	2	6	49,09	45,93	3	3	4	46,29	46,21
8	8	10	37,09	38,04	7	2	7	28,44	32,58	-1	6	2	46,99	46,36	2	3	4	46,04	47,28
8	4	10	33,22	28,26	6	2	7	72,75	73,45	2	1	6	33,92	36,53	2	4	3	39,65	37,83
8	3	10	74,60	76,05	-2	7	5	36,52	35,93	-1	-1	6	59,19	57,52	4	1	3	28,27	27,18
2	8	10	88,00	85,25	3	5	2	80,12	82,59	-1	1	6	25,92	20,92	3	1	4	36,93	36,29
7	6	10	49,46	46,46	-3	4	7	41,55	41,86	1	1	6	38,12	34,71	4	0	3	115,98	115,07
5	7	10	32,27	35,95	4	2	7	28,60	29,27	0	6	6	38,87	38,97	1	4	2	30,13	30,95
7	2	10	39,36	36,88	-2	3	7	26,30	25,33	0	6	5	24,85	27,38	1	2	4	26,71	30,63
7	0	10	38,50	37,26	-7	-3	3	35,94	32,93	0	5	6	24,77	26,11	1	1	4	19,70	15,99
4	6	10	45,75	47,27	2	3	7	52,14	55,09	0	4	4	64,83	66,23	1	4	0	88,66	88,83
6	2	10	50,90	50,90	-2	-2	7	40,23	35,88	0	3	6	43,07	43,48	1	0	4	197,26	193,33
1	8	10	32,89	33,39	7	2	2	24,81	14,56	0	6	3	30,14	30,29	-3	-3	1	25,10	20,39
0	8	10	51,23	51,11	1	7	7	68,30	64,77	-6	0	2	72,05	73,46	-2	-3	1	31,28	34,11
5	4	10	29,88	30,37	-1	7	6	31,74	32,08	-2	0	6	31,16	31,42	-3	-3	2	80,95	77,53
5	3	10	43,15	46,10	6	1	7	35,24	37,11	2	0	6	21,51	10,06	-3	-2	2	34,33	35,00
3	5	10	146,69	147,61	7	1	6	44,22	45,51	-1	6	0	49,62	46,91	-2	-3	2	35,24	31,75
5	1	10	47,73	51,40	-1	7	5	28,03	23,58	1	6	0	43,19	42,28	-2	-2	3	31,78	30,77
1	5	10	58,94	58,28	-1	5	7	146,83	148,56	0	0	6	105,51	103,76	-1	-3	2	19,82	18,49
5	0	10	40,80	46,86	1	7	5	51,68	54,05	-5	-3	5	47,19	43,18	-3	-1	2	34,75	32,93
0	5	10	42,66	42,68	1	5	7	54,69	55,41	-5	-1	5	32,60	30,86	-1	3	2	115,61	115,53
2	4	10	33,51	37,37	-1	6	7	48,96	48,68	-3	0	5	85,19	82,96	-1	2	3	154,31	148,70
1	4	10	64,30	67,67	-1	7	4	27,08	26,61	-5	-4	4	51,81	53,78	-1	-2	3	50,53	49,61
0	4	10	64,42	68,94	4	1	7	30,42	31,44	-4	-5	4	48,26	46,33	-2	-1	3	65,49	67,45
4	0	10	36,93	22,10	1	4	7	29,72	33,38	-4	-4	5	43,48	44,27	-1	3	3	23,33	21,36
3	2	10	29,30	25,10	-2	3	7	37,84	42,04	-5	-3	4	48,55	46,17	-3	-1	3	65,66	64,50
2	3	10	40,97	37,90	-7	-1	3	35,69	38,58	-3	-5	4	46,82	46,47	-1	3	1	66,89	65,50
1	3	10	33,30	38,40	-1	-1	7	30,83	32,93	-5	-4	3	68,79	65,59	-1	3	3	66,65	62,77
3	1	10	32,77	31,54	-1	7	3	53,66	55,38	-2	-5	4	33,59	28,78	0	-1	3	93,81	95,10
0	3	10	56,80	60,45	-1	-7	3	38,91	42,89	-2	-4	5	24,07	6,63	-1	-1	3	19,87	7,13
3	2	10	54,57	51,53	1	3	7	36,11	35,57	-5	-1	4	38,95	44,22	0	3	2	128,76	125,97
2	1	10	30,17	33,07	-7	-1	2	27,45	24,78	-5	0	4	26,17	23,50	0	2	3	55,48	55,93
1	2	10	57,13	57,63	-1	-2	7	58,90	58,86	-4	0	5	23,51	16,99	3	2	2	47,65	44,90
1	0	10	40,14	43,88	-2	1	7	59,68	61,44	-7	-1	3	37,01	35,87	3	3	3	64,83	68,13
0	1	10	107,86	107,14	-2	-1	7	70,91	66,30	-1	-3	5	118,00	115,46	1	3	2	120,56	123,62
9	9	9	39,61	47,10	-1	7	2	26,67	32,44	3	4	1	24,98	30,63	2	3	1	144,26	147,92
7	8	9	68,62	68,25	3	7	1	36,60	37,54	-1	5	3	43,69	45,66	1	1	3	159,67	155,93
6	8	9	38,50	35,84	-1	-1	7	66,07	64,31	-2	-3	5	41,26	42,62	1	3	0	145,70	149,54
8	5	9	37,71	38,94	-1	7	1	69,86	72,01	-3	1	5	47,81	47,57	1	0	3	72,54	67,22
5	8	9	85,48	85,73	0	7	7	56,18	56,39	-5	-2	3	29,39	29,11	0	0	3	77,24	75,09
4	8	9	30,63	28,69	0	6	7	53,42	58,01	-3	-5	3	90,35	90,08	-2	-1	2	35,45	31,95
3	8	9	28,41	25,35	5	0	7	73,45	74,03	0	-2	5	68,42	64,43	-1	-2	2	173,48	170,16
7	7	9	57,41	62,46	0	5	7	25,55	20,13	-2	-3	5	29,80	32,51	-1	2	2	82,97	78,92
6	7	9	52,72	53,23	7	0	4	35,82	37,05	-5	-2	2	36,19	35,72	-2	0	2	62,94	65,07
3	7	9	41,38	43,84	-7	0	3	37,30	32,59	-2	2	5	107,08	104,89	0	-2	2	65,29	65,07
6	5	9	117,51	119,11	0	-7	3	91,66	87,77	-1	5	0	94,10	93,19	-1	2	1	30,29	32,92
9	3	6	37,30	37,21	0	7	3	52,14	51,77	-1	0	5	61,95	62,14	-1	-1	2	106,91	103,54
4	9	9	39,81	38,07	0	3	7	53,37	52,51	-1	5	1	88,49	86,98	-1	2	0	39,86	38,97
9	5	2	86,47	85,64	-7	0	2	26,96	23,97	-1	1	5	78,52	76,31	0	2	0	28,40	30,02
4	2	9	79,96	80,87	-2	0	7	63,27	60,57	-1	-1	5	69,61	69,41	2	2	2	26,17	30,45
9	4	2	49,58	53,06	0	2	7	67,84	65,45	4	4	5	38,66	39,40	1	3	2	36,85	38,69
1	9	4	28,52	31,73	0	7	2	45,05	45,68	4	1	5	37,14	38,13	1	1	2	38,58	33,87
3	9	1	75,18	75,10	-1	0	7	67,59	68,03	5	3	4	44,76	46,82	2	1	2	45,75	47,47
9	3	2	56,55	54,72	6	6	6	208,80	220,75	2	5	4	28,11	29,69	0	2	2	138,69	138,64
1	1	9	66,36	63,62	4	6	6	62,90	65,93	1	2	5	103,49	105,38	0	1	2	46,24	48,20
7	5	8	36,64	31,34	8	6	5	44,60	42,44	2	3	5	20,73	20,60	0	2	1	38,50	38,69
9	6	8	36,36	32,52	6	4	5	106,67	107,65	1	5	4	40,64	39,42	0	0	2	26,30	30,02
6	8	5	30,71	32,52	5	4	6	91,66	90,69	1	4	5	312,46	315,02	-1	1	1	18,84	17,84
8	8	7	57,54	59,60	6	3	6	38,99	42,63	-5	-1	3	106,75	107,08					
4	7	8	104,65	106,89	-5	-6	1	30,42	31,28	-3	5	2	80,99	84,11					

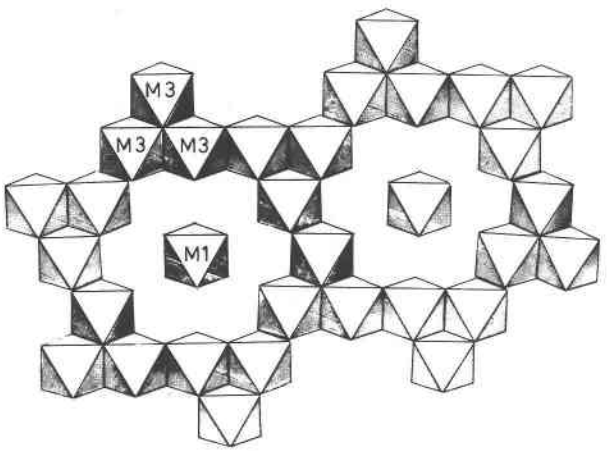

Fig. 1. Polyhedral representation of the metal atom $M(1)$, $M(3)$ arrangement between pairs of hexagonal stacked anion layers, viewed approximately down $[001]_{hex}$.

Composition—structure relationships

In the refinement of loveringite, electron-density and bond-length calculations indicated that a small amount of an atom both heavier and larger than Zr and Mg occurred together with these elements in the octahedral site $M(1)$. Also, when the unit-cell composition was expressed in terms of large cations A = Ca, REE, Pb, U, Th, Y, and small cations M = Ti, Fe, Cr, V, Zr, Mg, Al, Mn, a formula of $A_{1.10}M_{20.24}O_{38}$ was obtained. Accordingly, the excess A cations over those required to fill site $M(0)$ were ordered into site $M(1)$. Justification for this is found in a detailed electron-probe analysis for REE in loveringite (Campbell and Kelly, in press). The REE distribution pattern showed a maximum at La with a continuous decline to Eu, then a second build-up maximized at Ho, declining again to Lu. This unusual double-hump REE pattern suggests that REE are entering two distinct sites in the structure. The ionic radius of the La^{3+}, 1.32A, is very similar to that for Ca^{2+}, 1.35A, in 12-fold coordination (Shannon and Prewitt, 1969), and there is no doubt that the larger REE occupy site $M(0)$ in the anion framework, along with Ca. On the other hand, the ionic radius for Ho^{3+}, 0.894A, is virtually identical to that for Y^{3+}, 0.892A, in six-fold coordination. Yttrium is known to closely correlate with Zr in many mineral structures, and so the second REE enrichment, centered at Ho, is due to these smaller REE entering the $M(1)$ octahedral site, along with Zr and Y. It is highly likely that tetravalent Hf also occupies site $M(1)$, and the possibility of some tetravalent Ce, ionic radius = 0.80A, in this site cannot be discounted. The occupation of the $M(1)$ site by small REE also explains why davidites generally have more than one A cation per unit cell (*e.g.* see analytical data of Pabst, 1961). The chondrite-normalized REE distribution patterns for davidites show the same double-maxima as for loveringites (Campbell and Kelly, in press).

Another compositional complication in the loveringite structure was that the total number of small cations, ΣM = 20.34 (including 0.1 REE) was less than the number of occupied sites, 21. This most likely occurs because all iron was considered to be Fe^{3+}, all vanadium V^{5+}, *etc.*, in the reconstituted mineral. By analogy with reported chemical analyses on isostructural minerals, it is certain that, in the original crystal, these elements were at least partly present in their lower valence states. In the data crystal, for example, if one-third of the iron were ferrous, the calculated unit-cell composition would then have ΣM = 21 and there would be no vacancies in the small cation sites (assuming no other sites become occupied). Consistent with this interpretation, the vacancies were considered to be associated with those sites to which iron was assigned, *i.e.* $M(2)$ and $M(3)$.

A further structural variation in the loveringite samples is suggested by analyses for grains such as N138-17 and C187-31, Table 1. For the latter sample, the calculated unit-cell composition, normalized to 38 oxygens, is $[Ca_{1.34}REE_{0.05}(Y,Th,U,Pb)_{0.04}][Ti_{13.29}Fe_{4.32}V_{0.80}Al_{0.50}Mg_{0.27}Zr_{0.16}(Mn,Cr)_{0.08}]O_{38}$, *i.e.* $A_{1.43}M_{19.42}O_{38}$, where A is predominantly Ca. This large atom is unlikely to substitute into the octahedral site $M(1)$, and it is necessary to find an alternative site for the 0.43 A atoms above that required to fill site $M(0)$. A likely possibility is that the extra A occupies the remaining anion site on the trigonal axis [two-fold site O(7) in Table 2]. The formula may then

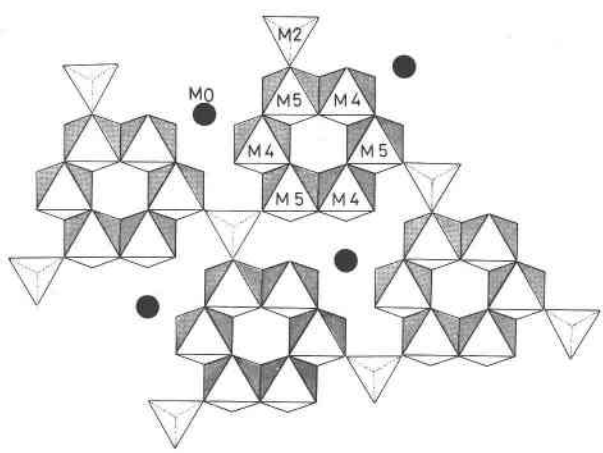

Fig. 2. Polyhedral representation of the metal atom $M(2)$, $M(4)$, $M(5)$ arrangement between hexagonal- and cubic-stacked anion layers, viewed down $[001]_{hex}$. The filled circles represent calcium.

be generalized as $A_{3-x}\square_x M_y O_{36}$ where $\square$ = vacancy, *i.e.* it is assumed that both A cations and oxygen anions cannot both occupy the same anion site. In this situation there are no oxygens on the three-fold axis, a situation suggested by Pabst (1961) for the isotypic mineral davidite. Pabst used chemical analyses (including valence-state determinations for iron) and specific gravity data to determine unit-cell com-

Table 4. Loveringite—interatomic distances (A) and angles (°)

		Distance	O-M-O angle
M(1) octahedron			
M(1) - O(1)	[6]	2.166*	
O(1) - O(1)^1	[6]	3.01	88.16*
- O(1)^{11}	[6]	3.11	91.84
M(3) octahedron			
M(3) - O(4)		1.935	
- O(3)		1.972	
- O(2)		1.973	
- O(4)^1		1.987	
- O(7)		1.990	
- O(2)^1		2.039	
O(4) - O(4)^1		2.65	85.14
- O(2)		2.70	84.13
O(7) - O(2)		2.64	82.06
- O(2)^1		2.64	83.73
O(2) - O(2)^1		2.76	86.74
O(4) - O(7)		2.79	89.20
- O(3)		2.82	90.93
- O(2)^1		2.87	92.27
O(4) - O(3)		2.82	92.47
O(3) - O(7)		2.87	92.71
- O(2)		2.97	97.61
O(4)^1 - O(2)^1		3.02	101.10

		Distance	O-M-O angle
M(2) tetrahedron			
M(2) - O(5)	[3]	1.977	
- O(7)		2.047	
O(5) - O(5)^1	[3]	3.28	112.32
- O(7)	[3]	3.22	106.44
M(4) octahedron			
M(4) - O(2)		1.878	
- O(1)		1.992	
- O(3)		1.960	
- O(6)		1.934	
- O(5)		2.000	
- O(6)^1		2.060	
O(1) - O(6)		2.63	80.87
O(5) - O(3)		2.57	80.77
- O(6)		2.59	82.30
- O(1)		2.70	84.93
O(2) - O(6)		2.75	88.38
O(1) - O(3)		2.86	92.55
O(6) - O(6)^1		2.82	89.71
O(2) - O(1)		2.87	95.88
- O(3)		2.89	97.65
- O(6)		2.86	97.17
O(6)^1 - O(3)		2.88	95.40
- O(5)		2.95	93.27

		Distance	O-M-O angle
M(0) Site			
M(0) - O(2)	[6]	2.772	
- O(6)	[6]	2.807	
O(2) - O(6)	[6]	2.75	59.01
O(2) - O(2)	[6]	2.76	59.61
O(6) - O(6)	[6]	2.82	60.27
O(2) - O(6)^1	[6]	2.86	61.66
M(5) octahedron			
M(5) - O(1)		1.895	
- O(4)		1.877	
- O(3)		1.908	
- O(5)		1.984	
- O(6)		2.038	
- O(5)^1		2.120	
O(5) - O(5)^1		2.55	76.80
- O(3)		2.57	78.94
O(6) - O(1)		2.63	83.78
- O(5)		2.59	80.12
O(1) - O(5)		2.80	88.39
O(4) - O(6)		2.79	90.76
O(3) - O(5)^1		2.82	92.77
- O(4)		2.84	97.11
O(1) - O(4)		2.86	98.69
- O(3)		2.93	100.99
O(5)^1 - O(4)		2.90	97.13
- O(6)		3.00	92.53

Metal-Metal distances**

M(1) - M(5)	c	3.629
- M(4)	c	3.796
M(3) - M(3)^1	e	2.888
- M(3)^{11}	e	2.989
- M(5)	e	3.371
- M(4)	c	3.440
- M(5)^1	c	3.468
- M(4)^1	c	3.524
- M(5)^{11}	c	3.592
- M(4)^{11}	c	3.543
M(2) - M(5)	c	3.363
- M(5)^1	c	3.485
- M(4)	c	3.493
M(4) - M(5)	e	2.994
- M(5)^1	e	3.054
M(4) - M(4)	c	3.963
M(0) - M(4)	c	3.365
M(5) - M(5)	e	3.217

**Standard deviations for M-M, M-O and O-O are 0.004, 0.011 and 0.015 Å respectively and for angle O-M-O 0.4 degrees.*

***c and e refer to corner- and edge-shared linkages.*

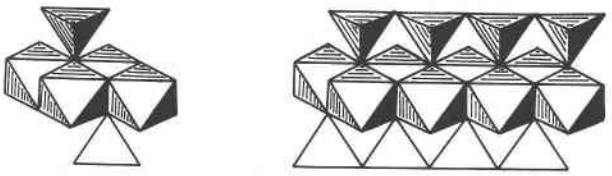

(i) (ii)

Fig. 3. (i) Representation of articulation of $M(4)O_6$, $M(5)O_6$, and $M(2)O_4$ polyhedra between adjacent h–M–c layers in loveringite. (ii) Basic structural element in $Ga_4Ti_{21}O_{48}$ (Lloyd *et al.*, 1976).

positions for davidite samples, and consistently obtained between 35 and 36 oxygens per unit cell. If the composition of loveringite sample C187-31 is normalized to 36 oxygens, we obtain $A_{1.35}M_{18.40}O_{36}$. This formula has considerably less than 21 M cations. The above hypothesis is consistent with the decreased number of M cations; atoms in sites $M(2)$ and $M(3)$ bond to anion O(7), and if O(7) is occupied by calcium, then sites $M(2)$ and $M(3)$ will be empty. However, where a vacancy occurs in anion site O(7), site $M(3)$ *may* be occupied by ions which can adapt to the reduced anion coordination, six-fold → five-fold. It is apparent that further structural work on davidites or high-calcium loveringites is necessary to clarify this question.

Systematic nomenclature of crichtonite-group minerals

A number of minerals have been reported in the literature which all have the same basic structure type as crichtonite, and similar compositions. According to Strunz (1966), these are davidite, crichtonite, senaite, and mohsite. In a recent composition and structural study, we find that the mineral landauite (Portnov *et al.*, 1966) also fits into this category (Grey and Gatehouse, 1978). All these minerals have trigonal symmetry and structures based on a close-packed-anion lattice with a nine-layer ($hhc\cdots$) stacking sequence along the trigonal axis. This complicated stacking sequence is apparently stabilized by the presence of large cations in sites in the cubic-stacked anion layers, *i.e.* the large cations are the structure-determining species, and we have proposed a nomenclature system for these isotypic minerals based on the *dominant* large cation in each case. This proposal is in harmony with the known compositions of the previously-named minerals from the type localities, and results in the following classification:

Mineral name	*Dominant large cation*
crichtonite	strontium
senaite	lead
davidite	REE
landauite	sodium
loveringite	calcium

Based on this proposal, loveringite then qualifies as a new member of the group, with calcium as the dominant large cation (Kelly *et al.*, 1978).

Acknowledgments

We wish to thank Dr. Henri-Jean Schubnel, Museum National d'Histoire Naturelle, Paris, for kindly supplying a sample of mohsite (Le Plate Muratouse, La Grave, Hautes Alpes, France, No. 103, 523).

References

Bannister, F. A. and J. E. T. Horne (1950) A radioactive mineral from Mozambique related to davidite. *Mineral. Mag., 29,* 101–112.

Baur, W. H. (1961) Atomabstände und Bindungswinkel im Brookit, TiO_2. *Acta Crystallogr., 14,* 214–216.

Campbell, I. H. and P. Kelly (1977) The geochemistry of loveringite. *Mineral. Mag.*, in press.

———, G. J. H. McCall and D. S. Tyrwhitt (1970) The Jimberlana norite, Western Australia—a smaller analogue of the Great Dyke of Rhodesia. *Geol. Mag., 107,* 1–12.

Geller, S. (1960) Crystal structure of β-Ga_2O_3. *J. Chem. Phys., 33,* 676–684.

Grey, I. E. and D. J. Lloyd (1976) The crystal structure of senaite. *Acta Crystallogr., B32,* 1509–1513.

——— and B. M. Gatehouse (1978) The crystal structure of landauite, $Na[MnZn_2(Ti,Fe)_6Ti_{12}]O_{38}$. *Can. Mineral.*, in press.

———, ———, and J. S. White, Jr. (1976) The structure of crichtonite and its relationship to senaite. *Am. Mineral., 61,* 1203–1212.

Hey, M. H., P. G. Embrey and E. E. Fejer (1969) Crichtonite, a distinct species. *Mineral. Mag., 37,* 349–355.

Hornstra, J. and B. Stubbe (1972) PW 1100 Data Processing Program, Philips Research Labs., Eindhoven.

Kelly, P., Ian H. Campbell, Ian E. Grey and Bryan M. Gatehouse (1978) Loveringite, $[Ca,REE][Ti,Fe^{3+},Cr]_{21}O_{38}$, a new mineral from Norseman, Western Australia. *Can. Mineral.*, in press.

Kleeman, J. D. and J. F. Lovering (1967) Uranium distribution in rocks by fission-track registration in lexan plastic. *Science, 156,* 512–513.

Lacroix, A. (1901) *Minéralogie de la France et de ses Colonies,* Vol. 3. Librairie Polytechnique, Paris.

Levy, A. (1827) On a new mineral species. *Phil. Mag.*, ser. 2, *1,* 221–223.

Lloyd, D. J., I. E. Grey and L. A. Bursill (1976) The structure of $Ga_4Ti_{21}O_{48}$. *Acta Crystallogr., B32,* 1756–1761.

Pabst, A. (1961) X-ray crystallography of davidite. *Am. Mineral., 46,* 700–718.

Portnov, A. M. L. Ye Nikolayeva and T. I. Stolyarova (1966) A new titanium mineral, landauite. *Doklady Akademii Nauk SSR, 166,* 1420–1421.

Shannon, R. D. and C. T. Prewitt (1969) Effective ionic radii in oxides and fluorites. *Acta Crystallogr., B25,* 925–946.

Strunz, H. (1966) *Mineralogische Tabellen,* 4th ed. Akademische Verlagsgesellschaft, Leipzig.

Manuscript received, April 25, 1977; accepted for publication, August 11, 1977.